

**Figure S1. The reduced pathogen resistance is not likely due to the impaired anabolism of PI(4,5)P2 and clathrin-mediated endocytosis.**

(A) Survival of wild-type, *arf-6(tm1447)*, and *amph-1(tm1060)* animals exposed to *P. aeruginosa*. The p-values for the comparisons are indicated (log-rank test). Sample sizes and mean lifespan are shown in Table S2.

(B-B') Confocal images of wild-type and *rab-10(ok1494)* animals expressing the transcriptional reporter *irg-4p::gfp* exposed to the indicated conditions. Box and whiskers plots (n = 25 animals): 10th-90th percentile; dots, outliers; red midline, median of *wild-type* animals; boundaries, quartiles. The p-values for the comparisons are indicated (one-way ANOVA with Tukey's multiple comparisons test). Scale bar, 100  $\mu$ m.

(C) Survival of wild-type and *dpy-23(RNAi)* animals exposed to *P. aeruginosa*. The p-values for the comparisons are indicated (log-rank test). Sample sizes and mean lifespan are shown in Table S2.

(D) A schematic representation of the adult worm intestine in confocal imaging is presented, with the imaging plane close to the basal membrane of the intestinal cells designated as "Top", and the imaging plane where the apical membrane and lumen can be seen labeled as "Middle" (deep cytosol).

(E-F') Screening of nine reported RAB-10 effectors using PI(4,5)P2 reporter Tubby-PH<sup>(R332H)</sup>::GFP and DAG reporter NES::GFP::C1ab-PKD1<sup>SC KI</sup>. Box and whiskers plots (n = 24 animals): 10th-90th percentile; dots, outliers; red midline, median of wild-type; boundaries, quartiles. The p-values for the comparisons are indicated (one-way ANOVA with Dunnett's multiple comparisons test). Scale bars, 10  $\mu$ m.

**Figure S2. Loss of UNC-16 leads to the aggregation of sorting endosomal structures.**

(A) Western blot showing UNC-16 expression in wild-type and *unc-16(e109)* animals.

**(B)** The membrane-to-cytosol ratio (P/S) of RAB-10 in wild-type and *unc-16(e109)* animals was measured. RAB-10 in the supernatants and pellets was analyzed by western blotting using an anti-GFP antibody. The loading control was blotted with the anti- $\beta$  actin antibody. The average P/S ratio was calculated by normalizing the intensity of the supernatant or pellet with the corresponding  $\beta$ -actin, and the ratios are presented beneath the blots.

**(C-C')** Confocal images showing the localization of RAB-5 in wild-type and *unc-16(e109)* animals. Box and whiskers plots (n = 24 regions): 10th-90th percentile; dots, outliers; red midline, median of wild-type; boundaries, quartiles. The p-value for the comparison is indicated (two-tailed, unpaired t-test). Scale bars: 10  $\mu$ m.

**(D)** The membrane-to-cytosol ratio (P/S) of RAB-5 in wild-type and *unc-16(e109)* animals was measured. RAB-5 in the supernatants and pellets was analyzed by western blotting using an anti-GFP antibody. The loading control was blotted with the anti- $\beta$  actin antibody. The average P/S ratio was calculated by normalizing the intensity of the supernatant or pellet with the corresponding  $\beta$ -actin, and the ratios are presented beneath the blots.

**(E')** Confocal images showing the colocalization (upper panels: Z-axis focal plane; lower panels: Y-axis focal plane) between UNC-16 and ARF-6::GFP or GFP::RAB-7. The DAPI channel (blue color) indicates broad-spectrum intestinal autofluorescence. Mander's coefficients were calculated using the Z-stack confocal slices. The data is the mean with 95% confidence intervals (n=9 animals). Scale bars: 10  $\mu$ m.

**Figure S3. An absence of UNC-16 induces an upsurge in endosomal PI(4,5)P2.**

**(A-B')** Confocal images showing the localization of Tubby-PH<sup>(R332H)</sup>::GFP and NES::GFP::C1ab-PKD1<sup>SC KI</sup> in wild-type, UNC-16::MC, or MC:RAB-10(Q68L) animals. Box and whiskers plots (n = 24 regions): 10th-90th percentile; dots, outliers; red midline, median of wild-type; boundaries, quartiles. The p-values for the comparison are indicated (two-tailed, unpaired t-test). Scale bars: 10  $\mu$ m.

(C) Survival of wild-type, UNC-16::MC, and MC:RAB-10(Q68L) animals exposed to *P. aeruginosa*. The p-values for the comparisons are indicated (log-rank test). Sample sizes and mean lifespan are shown in Table S2.

(D-E') Confocal images showing the localization of Tubby-PH<sup>(R332H)</sup>::GFP and GFP::RME-1 in wild-type, *unc-16(e109)*, *arf-16(tm1447)*, and *arf-16(tm1447);unc-16(e109)* animals. Box and whiskers plots (n = 24 regions): 10th-90th percentile; dots, outliers; red midline, median of wild-type; boundaries, quartiles. The p-values for the comparison are indicated (one-way ANOVA with Tukey's multiple comparisons test). Scale bars: 10  $\mu$ m.

(F) The occupancy of wild-type, *rab-10(ok1494)*, and *unc-16(e109)* animals on a lawn of *P. aeruginosa* was measured. The data points represent the average of three replicates, and the error bars indicate 95% confidence intervals. The p-values for the comparisons are shown (one-way ANOVA with Sidak's multiple comparisons test).

#### **Figure S4. EGL-8/PLC- $\beta$ is essential for the hydrolysis of endosomal PI(4,5)P2**

(A-C') Confocal images showing the localization of Tubby-PH<sup>(R332H)</sup>::GFP, hTAC::GFP, and NES::GFP::C1ab-PKD1<sup>SC KI</sup> within cells after RNAi-mediated knockdown of 13 phospholipases, with *unc-16(RNAi)* as the phenotypical reference. Box and whiskers plots (n = 24 regions): 10th-90th percentile; dots, outliers; red midline, median of wild-type; boundaries, quartiles. The p-values for the comparison are indicated (one-way ANOVA with Dunnett's multiple comparisons test). Scale bars: 10  $\mu$ m.

#### **Figure S5. EGL-8/PLC- $\beta$ specifically interacts with UNC-16 and is involved in the hydrolysis of endosomal PI(4,5)P2.**

(A) Co-immunoprecipitation assays were performed using animals expressing epitope-tagged EGL-8 and RAB-10. IB, immunoblot; IP, immunoprecipitation; MC, mCherry.

(B) Western blot showing the interaction between RAB-10, loaded with either GTP $\gamma$ S

or GDP, and *in vitro* translated HA-tagged EGL-8.

(C) Western blot showing GST pull-down with *in vitro* translated HA-tagged PLC-1, PLC-2, PLC-3, and PLC-4.

(D-D') Confocal images showing the localization of Tubby-PH<sup>(R332H)</sup>::GFP in wild-type, *unc-16(e109)*, *unc-16(e109);EGL-8::MC(OE)*, *unc-16(e109);PLC-1::MC(OE)*, *unc-16(e109);PLC-2::MC(OE)*, *unc-16(e109);PLC-3::MC(OE)*, and *unc-16(e109);PLC-4::MC(OE)* animals. Box and whiskers plots (n = 24 regions): 10th-90th percentile; dots, outliers; red midline, median of wild-type; boundaries, quartiles. The p-values for the comparison are indicated (one-way ANOVA with Dunnett's multiple comparisons test). MC, mCherry. Scale bars: 10  $\mu$ m.

**Figure S6. EGL-8 is essential for the RAB-10-mediated innate immune response.**

(A) Survival of wild-type, *rab-10(ok1494)*, and *rab-10(ok1494);EGL-8::mCherry(OE)* animals was examined when exposed to *P. aeruginosa*. The p-values for the comparisons are indicated (log-rank test). Sample sizes and mean lifespan are shown in Table S2.

(B-B') Confocal images of wild-type, *rab-10(ok1494)*, and *rab-10(ok1494);EGL-8::mCherry(OE)* animals expressing the transcriptional reporter *irg-4p::gfp* after exposure to *P. aeruginosa*. Box and whiskers plots (n = 25 animals): 10th-90th percentile; dots, outliers; red midline, median of *wild-type* animals; boundaries, quartiles. The p-values for the comparisons are indicated (one-way ANOVA with Tukey's multiple comparisons test). Scale bar, 100  $\mu$ m.

**Figure S7. Overexpression of UNC-16(L360P) failed to restore the subcellular localization of Tubby-PH<sup>(R332H)</sup>, hTAC::GFP, and EGL-8::GFP<sup>SC KI</sup> in UNC-16-deficient animals, and the mRNA level of TBC-11 was not affected by *P. aeruginosa* infection.**

(A-C') Confocal images showing the localization of Tubby-PH<sup>(R332H)</sup>::GFP, hTAC::GFP, and EGL-8::GFP<sup>SC KI</sup> in wild-type, *unc-16(e109)*, *unc-16(e109);UNC-16::mCherry(OE)*, and *unc-16(e109);UNC-16(L360P)::mCherry(OE)* animals. Box and whiskers plots (n = 24 regions): 10th-90th percentile; dots, outliers; red midline, median of wild-type; boundaries, quartiles. The p-values for the comparison are indicated (one-way ANOVA with Dunnett's multiple comparisons test). Scale bars: 10  $\mu$ m.

(D) qPCR analysis evaluating the expression of *tbc-11* before and after exposure to *P. aeruginosa*. The data were the mean  $\pm$  SEM of three replicates. The p-value for the comparison is indicated (two-tailed, paired t-test).

**Figure S8. The upregulation of LET-413 in response to *P. aeruginosa* infection is contingent upon the presence of NHR-25.**

(A-A') Confocal images showing the localization of endogenous UNC-16 in the absence or presence of *P. aeruginosa*. Box and whiskers plots (n = 24 regions): 10th-90th percentile; dots, outliers; red midline, median of wild-type; boundaries, quartiles. The p-value for the comparison is indicated (two-tailed, unpaired t-test). Scale bars, 10  $\mu$ m.

(B-B') Western blot showing the endogenous levels of UNC-16. The relative intensity of UNC-16 was quantified relative to actin. The data were the mean  $\pm$  SEM of three replicates. The p-value for the comparison is indicated (two-tailed, paired t-test).

(C-C') Confocal images showing the localization of EGL-8::GFP<sup>SC KI</sup> in the absence or presence of *P. aeruginosa*. Box and whiskers plots (n = 24 regions): 10th-90th percentile; dots, outliers; red midline, median of wild-type; boundaries, quartiles. The p-value for the comparison is indicated (two-tailed, unpaired t-test). Scale bars, 10  $\mu$ m.

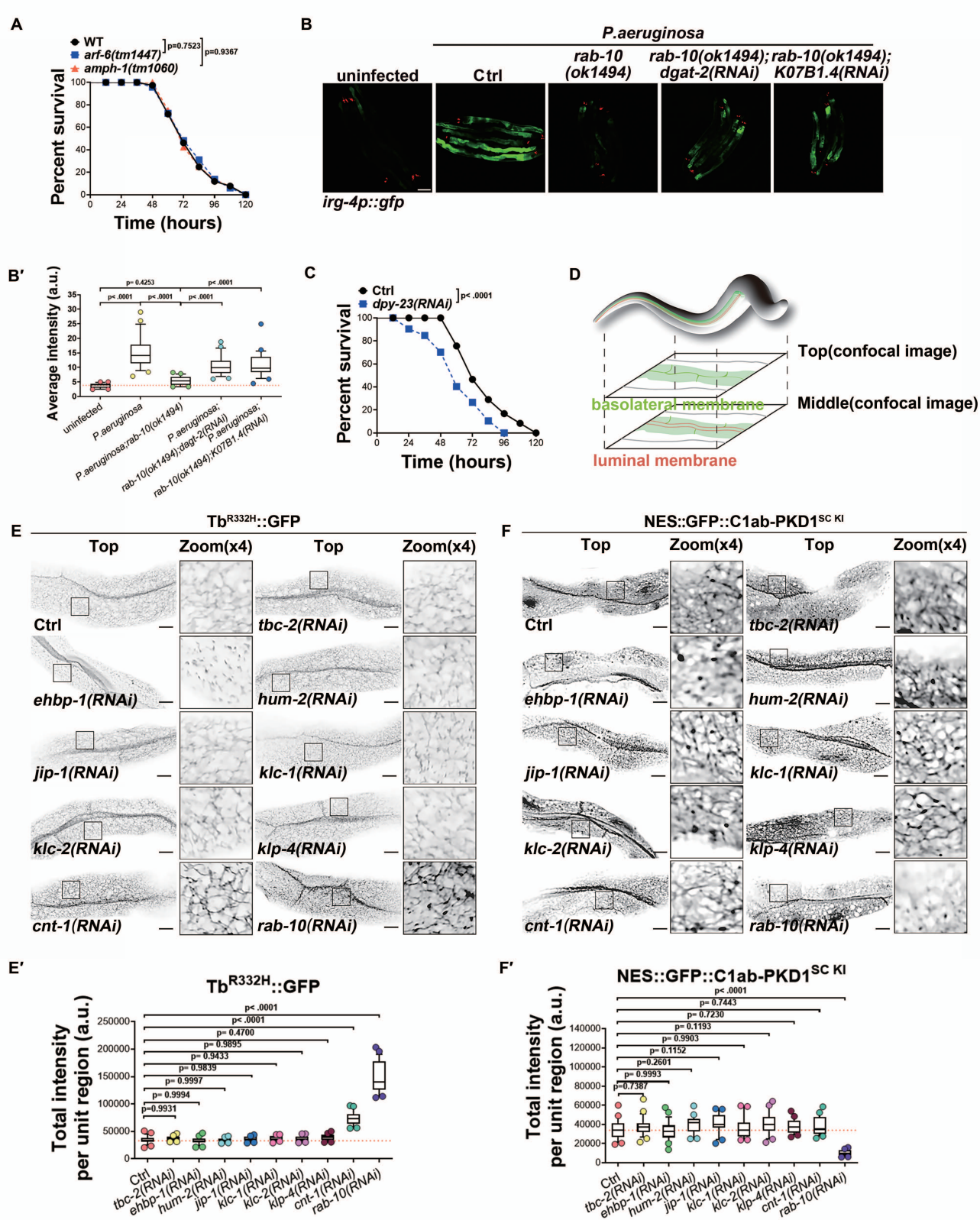
**(D-D')** Western blot showing the endogenous levels of EGL-8. The relative intensity of EGL-8 was quantified relative to actin. The data were the mean  $\pm$  SEM of three replicates. The p-value for the comparison is indicated (two-tailed, paired t-test).

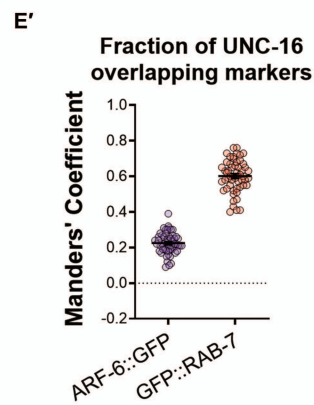
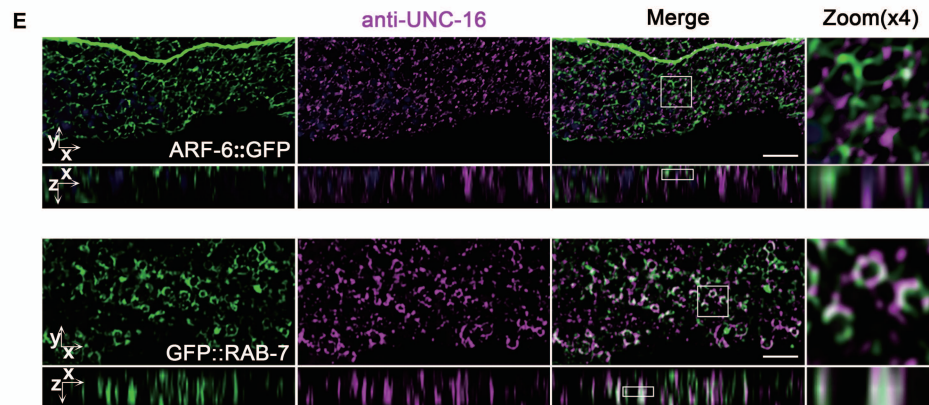
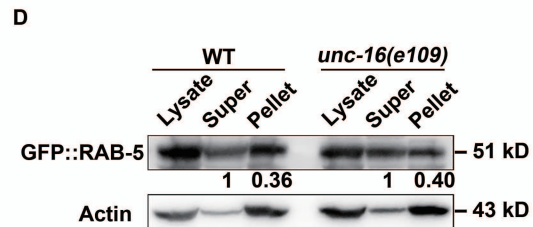
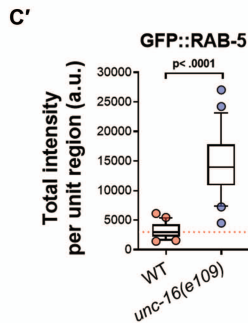
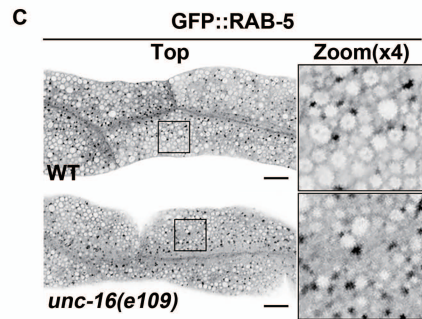
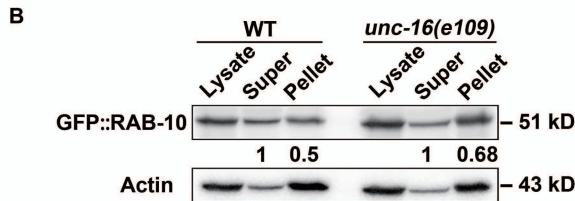
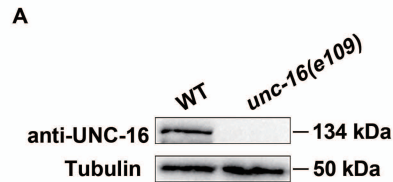
**(E)** qPCR analysis evaluating the expression of *unc-16* and *egl-8* before and after exposure to *P. aeruginosa*. The data were the mean  $\pm$  SEM of three replicates. The p-values for the comparison are indicated (one-way ANOVA with Dunnett's multiple comparisons test).

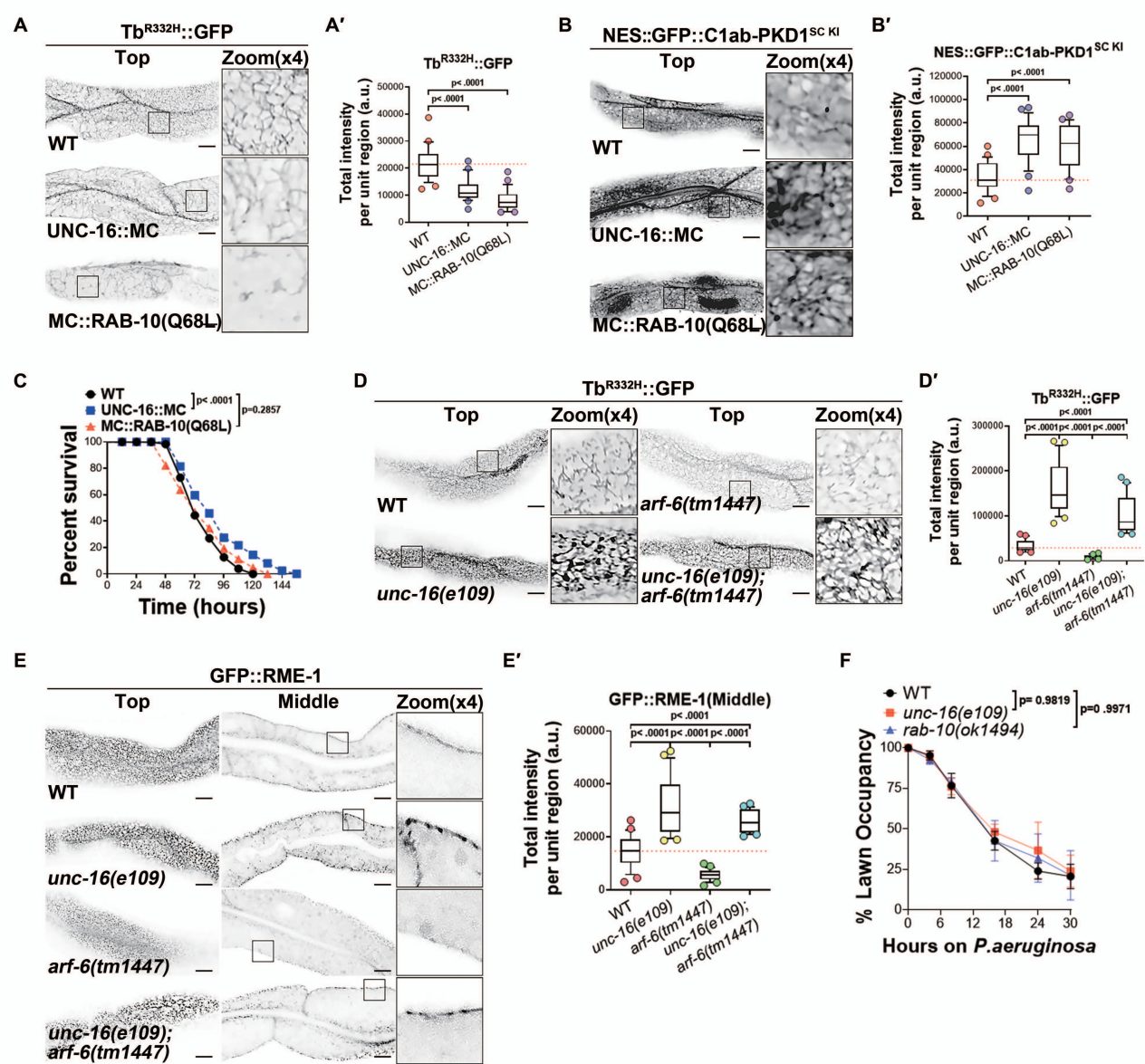
**(F-F')** Confocal images showing the localization of endogenous RAB-10 in the absence or presence of *P. aeruginosa*. Box and whiskers plots (n = 24 regions): 10th-90th percentile; dots, outliers; red midline, median of wild-type; boundaries, quartiles. The p-values for the comparison are indicated (one-way ANOVA with Dunnett's multiple comparisons test). Scale bars, 10  $\mu$ m.

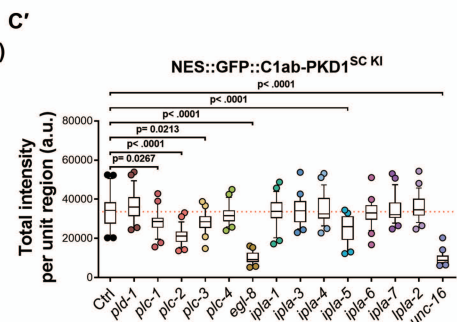
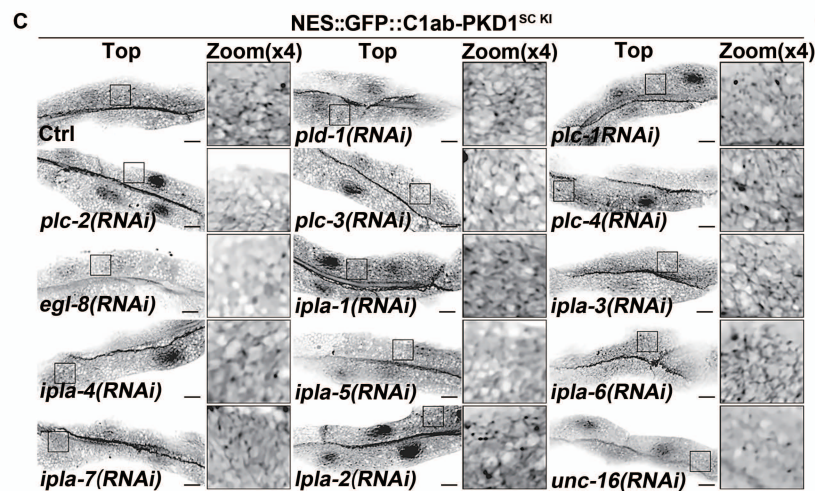
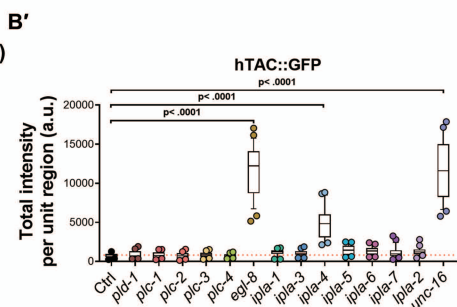
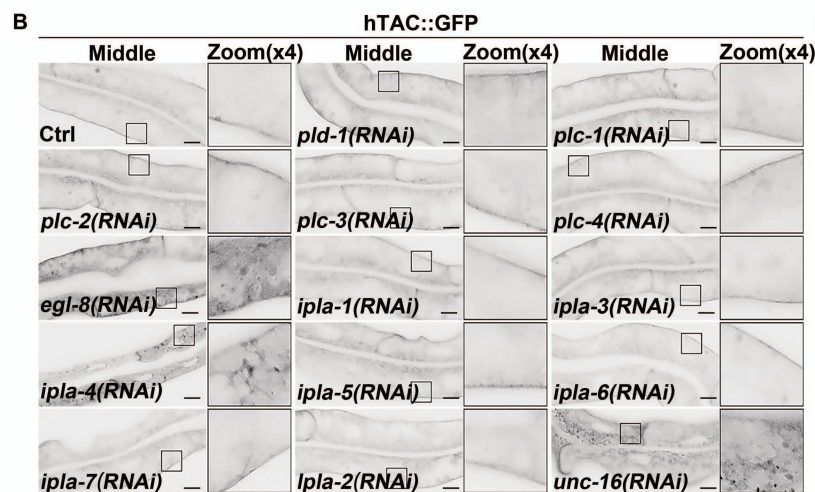
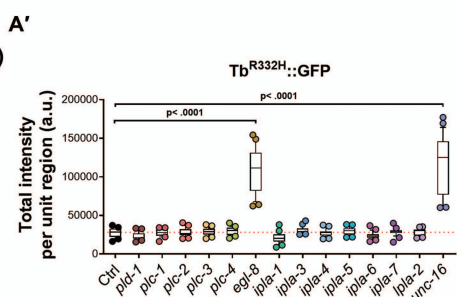
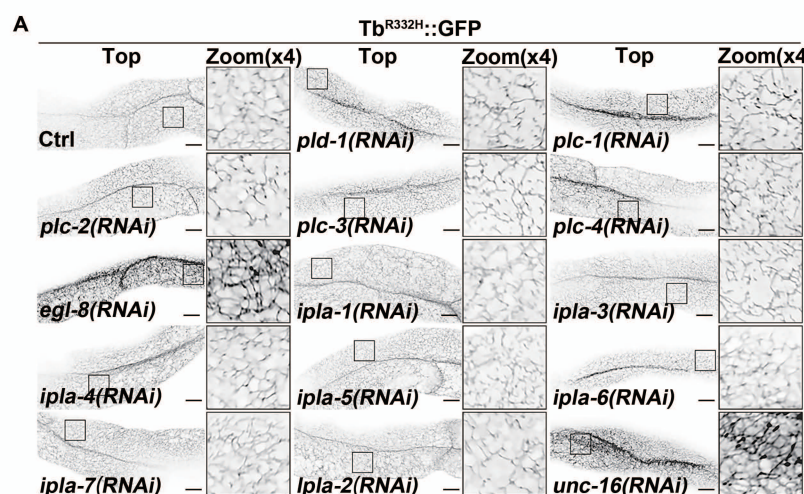
**(G)** Western blot showing the endogenous levels of RAB-10. The relative intensity of RAB-10 was quantified relative to actin. The ratios have been provided beneath the blots.

**Figure S9.** A model illustrating that in the intestine of *C. elegans*, RAB-10 mediates the hydrolysis of endosomal PI(4,5)P<sub>2</sub>, which is essential for developing immunity to pathogens. The amplified RAB-10 activity, due to *P. aeruginosa* infection, could be attributed to an increase in LET-413 expression, which is regulated by the nuclear receptor family transcription factor NHR-25.

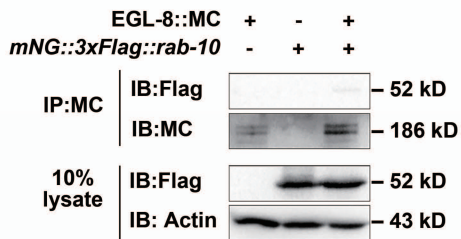




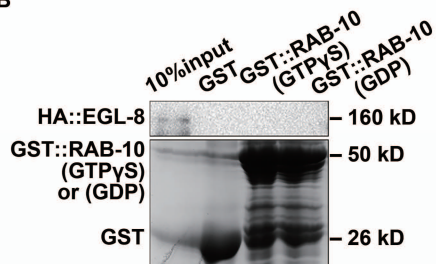




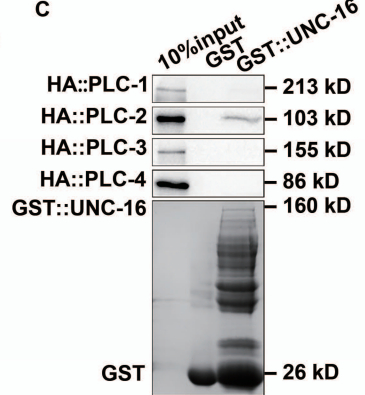
A



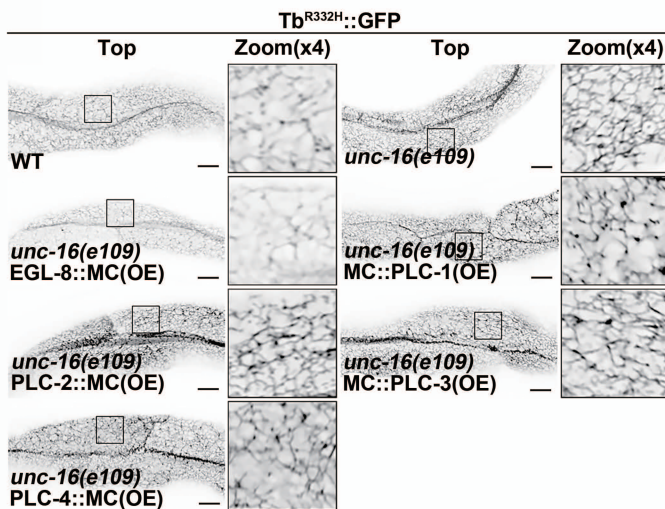
B



C



D



D'

